

High-efficiency photon-number-resolving multichannel detector

Michal Mičuda,¹ Ondřej Haderka,^{1,2} and Miroslav Ježek^{1,*}

¹*Department of Optics, Faculty of Science, Palacký University, 17. listopadu 50, 77200 Olomouc, Czech Republic*

²*Joint Laboratory of Optics, Palacký University and Physics Institute of Academy of Sciences of the Czech Republic,*

17. listopadu 50A, 77200 Olomouc, Czech Republic

(Received 9 April 2008; published 18 August 2008)

A balanced eight-port photon-number-resolving detector is developed. The employed scheme is based on an optical-fiber time-multiplexed device with the unique total optical transmittance reaching 93% and a pair of avalanche photodiodes. The balanced operation is achieved even for imperfect unbalanced fiber splitters used in the time-multiplexed device. The complete characterization of the detector for both classical and single-photon signals is presented. High-speed photon counting at the rates of 100 kHz with the total detection efficiency exceeding 50% is verified.

DOI: 10.1103/PhysRevA.78.025804

PACS number(s): 42.50.Ar, 03.67.-a, 85.60.Gz, 42.79.Sz

Photon-number-resolving detectors are capable of distinguishing the number of photons in an incident light mode. Detection with photon-number resolution represents a crucial technique for many quantum optics applications, especially in the emerging field of quantum information processing. The method of linear optical quantum computing [1,2], for example, relies fundamentally on the preparation and detection of single photons. Further, in quantum cryptography the quality of used single-photon states strongly affects the security of the transmission [3,4]. Single-photon states can be conditionally prepared using the process of parametric frequency down-conversion [5–9]. They have also been generated recently by single-photon emitters [10–15]. Successful high-fidelity conditional preparation of single-photon states and other nonclassical states as well as their characterization require detection with photon-number resolution. Particularly, in schemes without postselection, the precise knowledge of photon content is crucial. Unfortunately, common on-off photodetectors such as avalanche photodiodes and photomultiplier tubes are not able to distinguish among photon-number states, in particular between states of N and $N+1$ photons even for small N . Several strategies have been studied to reach the photon-number resolution, at least an approximate one in a limited range of photon numbers. The superconducting transition-edge sensors and quantum calorimeters [16,17], detectors based on atomic vapors [18,19], and visible light photon counters [20–22] represent several suggestions of detectors with an approximate photon-number resolution.

Using several on-off detectors without photon-number resolution, the photon-number resolving detector can be emulated. After dividing an incident light signal uniformly to several spatial modes, they can be detected by an array of on-off detectors [23–26]. An intensified charge-coupled device (CCD) camera has been recently used as the detector array in the limit of a large number of spatial modes [27]. The number of used on-off detectors can be reduced by means of time multiplexing instead of the spatial one. An initial light pulse is repeatedly split and delayed using either a storage loop and a single on-off detector [28–30] or a time-

multiplexed multichannel device and a pair of on-off detectors [31–33]. The compound detector retains the high quantum efficiency of commercially available on-off detectors reaching 75% [34] and yields an approximate photon-number resolution.

In the present paper, the photon-number resolving multichannel detector is developed adopting a technique of time multiplexing. The basic element of the design is a balanced splitting stage that divides an incident optical signal into two parts with the same energy. At the quantum level, the probabilities of a photon passing through the first channel and the second one are equal. After being divided, the signal is delayed in one channel by time delay τ . The splitting stage can be conveniently realized by a four-port (2×2) fiber splitter, where the signal is injected into one of its input ports. The first output port of the splitter is directly connected to the next splitting stage, while an optical fiber with a proper length is inserted at the output of the second port; see Fig. 1. The next splitting stage is constructed in the same way but with the time delay 2τ , i.e., using an optical fiber twice as long in one output port. Repeating the splitting stage m times, the $M=2^m$ distinct channels separated by time τ occur at the output of such a time-multiplexed multichannel device, one-half at the first output port of the last splitter and one-half at the second one. The signal at the output ports is detected by two on-off photodetectors with single-photon sensitivity. The optical delay line of the last stage can be replaced by electronic delay after photodetection.

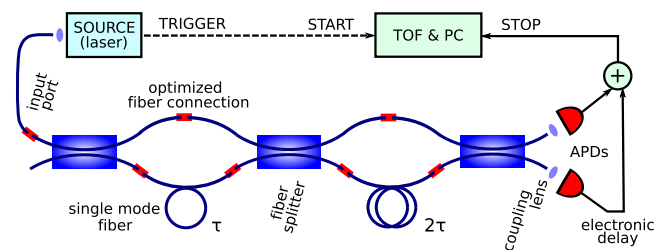


FIG. 1. (Color online) Scheme of the eight-port multichannel detector based on an optical-fiber time-multiplexed device and a pair of avalanche photodiodes (APDs). The device consists of three splitting stages realized using fiber splitters and single-mode fibers. See text for details.

*jezek@optics.upol.cz

The balanced operation of the multichannel detector important for the optimal measurement of unknown photon content [30] is not easy to achieve due to imperfections of commercially available fiber splitters, different insertion losses of fiber components employed in the time-multiplexed multichannel device, and different detection efficiencies of the on-off photodetectors. The balanced multichannel detector developed in this work is based on the time-multiplexed device design presented by groups of Walmsley and Franson [31–33]. Unlike the Walmsley-Franson scheme, the fiber splitters and other fiber components are used in a specific order and orientation that considerably improves the uniformity and makes the whole multichannel detector almost perfectly balanced even in the case of unbalanced fiber splitters and other mentioned imperfections. The uniformity of the multichannel detector is characterized by relative entropy,

$$S = \left(\ln \frac{1}{M} \right)^{-1} \sum_{k=1}^M p_k \ln p_k, \quad (1)$$

where p_k are relative probabilities of photon detection in individual output channels. A perfectly balanced multichannel detector yields the uniform probability $1/M$ of individual detection channels and thus $S=1$. The relative entropy determines a distance [35] between two probability distributions, namely, the true channel-probability distribution and the uniform one. Due to convexity of the distance, it possesses only one maximum, which significantly facilitates the optimization of the detector design and the comparison of different multichannel detectors. In this work, the optimal configuration is determined as the one with the maximal relative entropy (1), though other designs are possible depending on the application of the detector. Comparing the true probabilities of the channels and the ideal ones yields an alternative measure of the multichannel detector uniformity—the maximum relative deviation of channel probability,

$$\delta p = M \max_{k=1, \dots, M} \left| p_k - \frac{1}{M} \right|. \quad (2)$$

Besides the uniformity, the efficiency of detecting a photon by the multichannel detector represents another important parameter that is crucial especially for the detection of nonclassical light states. The total detection efficiency of the multichannel detector is given by the transmittance of the time-multiplexed multichannel device and by quantum efficiencies of the employed on-off photodetectors. The transmittance T of the multichannel device can be measured as a ratio of the total optical power in all output channels to the input optical power. Further, the average transmittance $T_{\text{stage}} = \sqrt[m]{T}$ of a splitting stage is defined, which facilitates the comparison of multichannel detectors with a different number of stages. The total detection efficiency of the multichannel detector can be alternatively determined by means of absolute calibration using correlated photon pairs produced by a nonlinear process of parametric frequency down-conversion [36–40].

The multichannel detector developed here consists of three splitting stages yielding $M=8$ channels. Nevertheless, it is easily scalable due to the stage topology. The fused 2

$\times 2$ single-mode fiber couplers designed for a wavelength of 830 nm with a typical relative deviation of 6% from an ideal balanced 50:50% splitting ratio (OZ Optics) are used for the splitting stages. The time delay between the channels is realized by 15- and 30-m-long single-mode optical fibers with a cutoff wavelength of 780 nm. The fibers are terminated by common ferrule connectors with physical contact (FC/PC) connectors. To achieve the minimum insertion losses of each fiber interconnection, the connector lock is removed and the connection is adjusted for the maximum power throughput. The output signal from the multichannel device is detected by two commercially available avalanche photodiodes (APDs) operated in Geiger mode with a typical dead time of 50 ns (Perkin Elmer SPCM-AQR-13-FC). Dark count rates and quantum efficiencies of the APDs are 150 s^{-1} , 120 s^{-1} and 58%, 55% at the wavelength of 825 nm, respectively. An electronic TTL signal from each APD consists of four channels separated by $\tau \approx 73$ ns. The signal from the second APD is delayed approximately by 37 ns with respect to the first one using the coaxial cable with a proper length. The output signals are summed yielding eight equidistant time channels.

The time-multiplexed multichannel device is characterized by measurements of the uniformity of the output channels and the total optical transmittance using strong coherent light signals. The laser diode (Sharp LT015) driven by a pulse generator (Avtech AVO-9A-C-EA-EW) serves as a source of input optical pulses with a wavelength of 824.5 nm at a 100 kHz repetition rate with a 4 ns pulse width. The average power of the source is stable within $\pm 0.01\%$ during a measurement run taking approximately one hour. The uniformity of the output channels is measured using a fast p - i - n photodiode (Thorlabs DET200) instead of the APDs connected to the multichannel device. A voltage from the photodiode coupled by a 50Ω load resistor is acquired by a digitizing oscilloscope (LeCroy WavePro 7200A) working in a memory segmentation regime. An area of each output pulse in the k th channel (segment) is measured and then statistically averaged over 10^4 input pulses. The normalized average pulse areas represent the probabilities of the output channels. The measurement yields the channel-probability distribution with entropy (1) of 0.999 ± 0.002 and the maximum relative deviation (2) of channel probability $\delta p = 0.13 \pm 0.01$. The total optical transmittance T of the multichannel device is determined by comparing the total output power and the input one measured by a power meter (Coherent FieldMaster GS) with a detection head (Coherent LM2) based on a silicon p - i - n photodiode. The detection head is placed instead of APDs and in the position of the first fiber connection at the input port (see Fig. 1) for the output and input power measurements, respectively. The power-meter is connected to a personal computer through RS232 serial interface and the measured power is recorded every 0.5 s for 2 min. The measured total optical transmittance $T = 0.9285 \pm 0.0002$ of the developed multichannel device can be directly compared with the similar three-stage multichannel device [31], which reaches a transmittance of 0.56 through an optical-fiber time-multiplexed system. The average transmittance of one splitting stage is 0.9756 ± 0.0001 in our case, which is the best result achieved so far to the best of our knowledge.

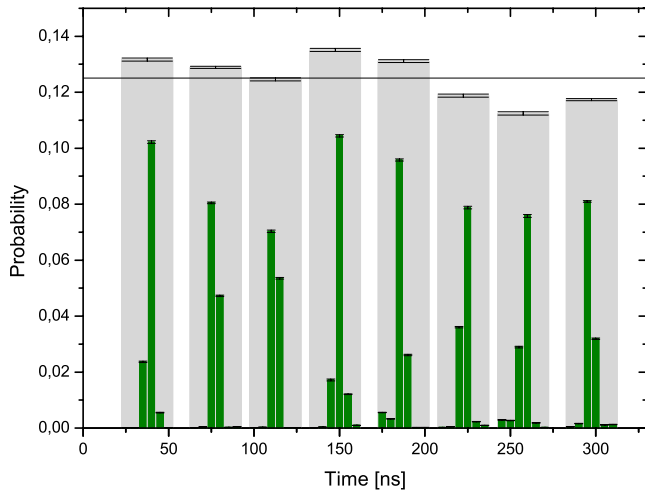


FIG. 2. (Color online) Measured response function of the time-multiplexed multichannel detector to weak light pulses; see text for details. The mean detection probabilities in 5 ns time bins (dark bars, green online) are clustered to form eight distinct detection channels (gray). Data standard deviations are shown as the corresponding error bars. The uniform $\frac{1}{8}$ probability distribution is plotted by a solid line (black).

Further, the uniformity of the whole photon-resolving multichannel detector is measured using a weak coherent light signal with Poissonian photon-number statistics. The laser-diode-based source of optical pulses is completed by two attenuators, the coarse mechanical attenuator (OZ Optics BB-200-33-830-S) and the precise digital one (OZ Optics DA100). The laser pulses are attenuated to a mean photon number of approximately one photon per pulse at the input port of the multichannel detector. There are equal probabilities of zero and one photon per pulse and multiphoton probability higher than 26%. The time-multiplexed multichannel-detector signal consisting of TTL pulses from the employed APDs is fed into the STOP input of the time-of-flight spectrometer (Fast ComTec TOF7885) that is connected to a personal computer through a multichannel buffer. The TRIGGER output of the laser-diode pulse generator serves as the START signal of the time-of-flight spectrometer. The STOP pulses are acquired during 1280-ns-long measurement sweeps with 5 ns time-bin resolution. The relative-frequency histogram of the events in the registered time bins is measured over 7×10^5 START pulses. The measurement run is repeated ten times, which yields a mean probability as well as a standard deviation of the detection probability in every time bin; see Fig. 2. The eight distinct well-separated detection channels are apparent in the time-of-flight data. The detection probabilities of the particular channel span several time bins due to the time jitter of the light source (0.5 ns), the jitter of the APDs ($\sqrt{2} \times 0.35$ ns), and to a large extent the time uncertainty of the time-of-flight spectrometer (2.5 ns) given as the half-width of the time bin. The total Gaussian width (rms) of about 2.6 ns of the detection channel corresponds well with the mentioned contributions. The mean probability of photon detection in the particular k th output channel is computed by summing the probabilities from six time bins around the corresponding center of gravity of the

channel positioned at time $(2.3+36.7k)$ ns, $k=1, \dots, 8$. The probabilities of the channels yield the entropy $S = 0.9991 \pm 0.0045$, and the maximum relative deviation (2) from the ideal uniform distribution reads $\delta p = 0.100 \pm 0.005$. A slightly better uniformity of the channel probabilities is reached in this case compared to the measurement of the multichannel device only (without APDs) using the strong light signal. It is an obvious consequence of considering the different quantum efficiencies of employed APDs in the entropy-maximization process described above. The resulting uniformity of the multichannel detector exceeds the uniformity of the devices presented recently [31–33]. The measured raw data can be further corrected to afterpulse probabilities [37], dark counts, and other imperfections. Such processing yields a small improvement of the multichannel detector uniformity comparable in size to the standard deviation of the measurement, and it is not presented here.

In conclusion, the photon-number-resolving multichannel detector based on an optical-fiber time-multiplexed device and two APD photodiodes working in on-off Geiger mode is presented. The detector yields eight almost perfectly balanced output channels with the maximum relative probability deviation of 10% from the target uniform distribution. The high uniformity of the detection channels has been reached in spite of employed imperfect unbalanced four-port (2×2) splitters and APDs with different responsivities. The total quantum efficiency of the multichannel detector is given by quantum efficiencies of used APDs and by the total optical transmittance of the multichannel device. The transmittance of $(92.85 \pm 0.02)\%$ has been measured, which yields the quantum efficiency of the whole multichannel detector exceeding 50%. Using carefully selected APDs with as high quantum efficiency as possible [34], the quantum efficiency of the multichannel detector can easily reach 65%. Thus, the detector can be directly used to generate and measure highly nonclassical states of light, for example, the photon-number Fock states and states with oscillating photon-number statistics. Further, the precise knowledge of the multiphoton content improves significantly the security of quantum cryptography protocols. Besides the efficiency, the response time and maximum possible repetition frequency are important for applications in optical communications. With a propagation delay of approximately 40 ns of the first detection channel and a jitter lower than 0.5 ns, the developed multichannel detector meets requirements of modern high-speed communication applications. The detector has been tested for an input pulse repetition frequency of 100 kHz, though it can work up to 3 MHz without any changes. The optical-fiber design of the time-multiplexed device can be further miniaturized and the whole multichannel detector can be on-chip integrated [41] yielding a compact photon-number-resolving detector.

This work was supported by Research Projects “Measurement and Information in Optics” (MSM 6198959213) and “Center of Modern Optics” (LC06007) of the Czech Ministry of Education. M.M. acknowledges also Grant No. GA202/05/0486 of GACR. O.H. acknowledges also Research Project 1M06002 of the Czech Ministry of Education.

- [1] E. Knill, R. Laflamme, and G. J. Milburn, *Nature (London)* **409**, 46 (2001).
- [2] J. D. Franson, M. M. Donegan, M. J. Fitch, B. C. Jacobs, and T. B. Pittman, *Phys. Rev. Lett.* **89**, 137901 (2002).
- [3] M. Dušek, M. Jahma, and N. Lütkenhaus, *Phys. Rev. A* **62**, 022306 (2000).
- [4] S. Félix, N. Gisin, A. Stefanov, and H. Zbinden, *J. Mod. Opt.* **48**, 2009 (2001).
- [5] C. K. Hong and L. Mandel, *Phys. Rev. Lett.* **56**, 58 (1986).
- [6] A. I. Lvovsky, H. Hansen, T. Aichele, O. Benson, J. Mlynek, and S. Schiller, *Phys. Rev. Lett.* **87**, 050402 (2001).
- [7] A. B. U'Ren, C. Silberhorn, K. Banaszek, and I. A. Walmsley, *Phys. Rev. Lett.* **93**, 093601 (2004).
- [8] A. B. U'Ren, C. Silberhorn, J. L. Ball, K. Banaszek, and I. A. Walmsley, *Phys. Rev. A* **72**, 021802(R) (2005).
- [9] E. Waks, E. Diamanti, and Y. Yamamoto, *New J. Phys.* **8**, 4 (2006).
- [10] C. Santori, D. Fattal, J. Vuckovic, G. Solomon, and Y. Yamamoto, *Nature (London)* **419**, 594 (2002).
- [11] M. Pelton, C. Santori, J. Vuckovic, B. Zhang, G. Solomon, J. Plant, and Y. Yamamoto, *Phys. Rev. Lett.* **89**, 233602 (2002).
- [12] A. Kuhn, M. Hennrich, and G. Rempe, *Phys. Rev. Lett.* **89**, 067901 (2002).
- [13] D. Englund, D. Fattal, E. Waks, G. Solomon, B. Zhang, T. Nakaoka, Y. Arakawa, Y. Yamamoto, and J. Vuckovic, *Phys. Rev. Lett.* **95**, 013904 (2005).
- [14] D. Press, S. Gotzinger, S. Reitzenstein, C. Hofmann, A. Löffler, M. Kamp, A. Forchel, and Y. Yamamoto, *Phys. Rev. Lett.* **98**, 117402 (2007).
- [15] T. Wilk, S. C. Webster, H. P. Specht, G. Rempe, and A. Kuhn, *Phys. Rev. Lett.* **98**, 063601 (2007).
- [16] B. Cabrera, R. M. Clarke, P. Colling, A. J. Miller, S. W. Nam, and R. W. Romani, *Appl. Phys. Lett.* **73**, 735 (1998).
- [17] D. Rosenberg, A. E. Lita, A. J. Miller, and S. W. Nam, *Phys. Rev. A* **71**, 061803(R) (2005).
- [18] A. Imamoglu, *Phys. Rev. Lett.* **89**, 163602 (2002).
- [19] D. F. V. James and P. G. Kwiat, *Phys. Rev. Lett.* **89**, 183601 (2002).
- [20] J. Kim, S. Takeuchi, Y. Yamamoto, and H. H. Hogue, *Appl. Phys. Lett.* **74**, 902 (1999).
- [21] S. Takeuchi, J. Kim, Y. Yamamoto, and H. H. Hogue, *Appl. Phys. Lett.* **74**, 1063 (1999).
- [22] E. Waks, K. Inoue, W. D. Oliver, E. Diamanti, and Y. Yamamoto, *IEEE J. Sel. Top. Quantum Electron.* **9**, 1502 (2003).
- [23] S. Song, C. M. Caves, and B. Yurke, *Phys. Rev. A* **41**, 5261 (1990).
- [24] H. Paul, P. Torma, T. Kiss, and I. Jex, *Phys. Rev. Lett.* **76**, 2464 (1996).
- [25] D. Mogilevtsev, *Opt. Commun.* **156**, 307 (1998).
- [26] P. Kok and S. L. Braunstein, *Phys. Rev. A* **63**, 033812 (2001).
- [27] O. Haderka, J. Peřina, Jr., M. Hamar, and J. Peřina, *Phys. Rev. A* **71**, 033815 (2005).
- [28] K. Banaszek and I. A. Walmsley, *Opt. Lett.* **28**, 52 (2003).
- [29] O. Haderka, M. Hamar, and J. Peřina, Jr., *Eur. Phys. J. D* **28**, 149 (2004).
- [30] J. Řeháček, Z. Hradil, O. Haderka, J. Peřina, Jr., and M. Hamar, *Phys. Rev. A* **67**, 061801(R) (2003).
- [31] D. Achilles, C. Silberhorn, C. Šliwa, K. Banaszek, and I. A. Walmsley, *Opt. Lett.* **28**, 2387 (2003).
- [32] M. J. Fitch, B. C. Jacobs, T. B. Pittman, and J. D. Franson, *Phys. Rev. A* **68**, 043814 (2003).
- [33] D. Achilles, C. Silberhorn, C. Šliwa, K. Banaszek, I. A. Walmsley, M. J. Fitch, B. C. Jacobs, T. B. Pittman, and J. D. Franson, *J. Mod. Opt.* **51**, 1499 (2004).
- [34] P. G. Kwiat, A. M. Steinberg, R. Y. Chiao, P. H. Eberhard, and M. D. Petroff, *Phys. Rev. A* **48**, R867 (1993).
- [35] S. Kullback and R. A. Leibler, *Ann. Math. Stat.* **22**, 79 (1951).
- [36] D. N. Klyshko, *Sov. J. Quantum Electron.* **10**, 1112 (1981).
- [37] P. G. Kwiat, A. M. Steinberg, R. Y. Chiao, P. H. Eberhard, and M. D. Petroff, *Appl. Opt.* **33**, 1844 (1994).
- [38] G. Brida, M. Genovese, M. Gramegna, M. L. Rastello, M. Chekhova, and L. Krivitsky, *J. Opt. Soc. Am. B* **22**, 488 (2005).
- [39] G. Brida, M. Genovese, I. Ruo-Berchera, M. Chekhova, and A. Penin, *J. Opt. Soc. Am. B* **23**, 2185 (2006).
- [40] S. V. Polyakov and A. L. Migdall, *Opt. Express* **15**, 1390 (2007).
- [41] A. Politi, M. J. Cryan, J. G. Rarity, S. Yu, and J. L. O'Brien, *Science* **320**, 646 (2008).